

Proceedings Article

A Novel Approach to FFL Trajectory Analysis

Frauke Niebel ^{a,b} · Jonas Schumacher ^a · Fabian Mohn ^{c,d} · Mandy Ahlborg ^a · Thorsten M. Buzug ^{a,b} · Matthias Graeser ^{a,b,*}

^aFraunhofer Research Institution for Individualized and Cell-Based Medical Engineering IMTE, Lübeck, Germany

^bInstitute of Medical Engineering, University of Lübeck, Lübeck, Germany

^cSection for Biomedical Imaging, University Medical Center Hamburg-Eppendorf, Hamburg, Germany

^dInstitute for Biomedical Imaging, Hamburg University of Technology, Hamburg, Germany

*Corresponding author, email: matthias.graeser@imte.fraunhofer.de

© 2023 Niebel *et al.*; licensee Infinite Science Publishing GmbH

This is an Open Access article distributed under the terms of the Creative Commons Attribution License (<http://creativecommons.org/licenses/by/4.0>), which permits unrestricted use, distribution, and reproduction in any medium, provided the original work is properly cited.

Abstract

The sampling trajectory is an important parameter of a magnetic particle imaging (MPI) system and should be selected in order to guarantee the best image quality constrained by hardware limitations. A simulation study is performed with the side conditions of a permanent magnet-based field-free line (FFL) scanner system evaluating multiple trajectory types (radial, spiral, uniform spiral, flower) and trajectory densities in terms of spatial resolution. The findings provide information on suitable FFL trajectories and indicate initial trends for advantageous sampling patterns in the reference system. While the study presented here uses simulated data, the used software framework has the potential to generate sequenced signals based on real measurement data. Within this framework, we present a novel approach to FFL trajectory analysis.

I. Introduction

In magnetic particle imaging (MPI) spatial encoding is realised by a selective low field region resembling a field-free point (FFP) or a field-free line (FFL). This region is translated through the field of view (FOV) on a sampling trajectory described by a spatial and time dependent field sequence [1]. Previously performed trajectory analysis showed that both the type and the density of the trajectory have a significant impact on the image properties demanding for a careful choice of the sampling pattern [2, 3]. In this work, a simulation study is carried out to assess selected trajectories for FFL MPI with regard to spatial resolution. The referenced scanner system features a permanent magnet generated FFL between two opposing Halbach dipole cylinders. The FFL is moved on a trajectory by means of an excitation drive field (DF) and a focus field (FF) as well as a mechanical rotation of the gantry [1]. In comparison to prior model-based

trajectory studies [2, 3], sequenced signals are calculated based on a custom simulation framework [4] that allows to include measured particle dynamics instead of complex particle models.

II. Methods and materials

The following two subsections briefly introduce the selected trajectories and the developed simulation approach, followed by an overview of the resolution analysis conducted in the scope of this study.

II.1. Trajectories for FFL MPI

In the analysis, a radial, a spiral, a uniform spiral and a flower trajectory (cf. Figure 1) are considered for different trajectory densities S and a constant scan time T . The trajectories are adopted from a similar study performed by Top *et al.* [2]. Each trajectory is defined by a relation

between the FF frequency f_{FF} and the rotation frequency of the FFL f_{rot} as well as a specific FF current waveform.

II.II. Simulation approach

The simulation approach is based on the core algorithm of a custom software framework [4] that allows for a measurement-based generation of sequenced signals. However, the input data used in this study is simulated by the Langevin theory in order to reduce complexity. A two dimensional data set contains the particle response to an one dimensional excitation field (drive field, DF) superimposed by a range of different DC-offsets in one direction. This resembles the response to an overlaying gradient field with an FFL which is subsequently transformed to resemble a specific particle response for a given field sequence. Thereby, the FF shifting can be mapped by means of a stepwise translation of a virtual FOV over the raw data set. The signals for a given focus field offset are obtained for all offset positions within the virtual FOV using linear interpolation. To map the rotation, the FOV is then rotated by an angle corresponding to the given point in time of the sequence. According to the FF current waveforms of the selected trajectories, the translation of the virtual FOV is defined being linear for the uniform spiral trajectory or sinusoidal for the other trajectory types. The transformation of the raw data yields a high resolution system matrix $\hat{\mathbf{S}}_{\text{HR}}$ (1 mT/ μ_0 steps in y -direction) and a low resolution system matrix $\hat{\mathbf{S}}_{\text{LR}}$ (1.25 mT/ μ_0 steps in y -direction) with a FOV of $200 \times 200 (\text{mT}/\mu_0)^2$. Different discretisation grids are used in order to avoid inverse crime, occurring when reusing the same model. All phantom signals are superimposed by a modelled $1/f$ noise representing realistic MPI receiver noise in the magnetic moment domain [4]. Images are reconstructed by the system matrix-based reconstruction approach using the iterative Kaczmarz method, implemented with a penalising parameter λ with Tikhonov regularisation [5].

II.III. Resolution analysis

In this study, spatial resolution is assessed by the modulation transfer function (MTF), that describes the contrast damping by the imaging process [6]. In order to determine the MTF, five software phantoms with a sinusoidal particle concentration $c(x) = 0.5 \cdot [1 + \sin(2\pi f_r x)]$ parallel to the x - or y -axis are used that feature different spatial frequencies f_r measured in line pairs (lp) per mT/ μ_0 ranging from 0.04 lp/(mT/ μ_0) to 0.08 lp/(mT/ μ_0). Firstly, the sine phantoms of all spatial frequencies are reconstructed for a given direction and trajectory. In a second step, an intensity profile is calculated for every reconstructed image by taking an average of three pixels left and right of the center line. A sampling point of the MTF can be calculated from the maximum (I_{max}) and

Table 1: Overview of the chosen frequencies (in Hz).

| S | Radial | | Spiral/Uniform Spiral | | Flower | |
|----|------------------|-----------------|-----------------------|--------------------------------------|------------------|-----------------|
| | f_{rot} | f_{FF} | f_{rot} | f_{FF} Or $1/T_{\text{FF}}$ | f_{rot} | f_{FF} |
| 4 | 5 | 20 | 20 | 5 | 25 | 20 |
| 8 | 5 | 40 | 40 | 5 | 45 | 40 |
| 12 | 5 | 60 | 60 | 5 | 65 | 60 |
| 16 | 5 | 80 | 80 | 5 | 85 | 80 |

minimum signal intensity (I_{min}) in the image

$$\text{MTF}(f_r) = \frac{I_{\text{max}} - I_{\text{min}}}{I_{\text{max}} + I_{\text{min}}}. \quad (1)$$

In order to assess the homogeneity of resolution, the MTF is determined in a rectangular central area centered around an offset of 0 mT/ μ_0 and a rectangular border area centered around an offset of 60 mT/ μ_0 . Since at least one maximum and one minimum of the sine wave must lie in the considered regions to determine the MTF, the width of the ranges is chosen to be 25 mT/ μ_0 according to the lowest spatial frequency. The resolution R is defined by the half of the value at which $\text{MTF}(1/R)$ equals 0.5 [6].

III. Experiments

For the simulation of the particle response by means of the Langevin theory, the following parameters were used: particle core diameter $D = 15.5$ nm, particle temperature $T_p = 310$ K, saturation magnetisation of magnetite $M_s = 0.6$ T/ μ_0 , iron concentration $c_{\text{Fe}} = 5$ $\mu\text{g}/\mu\text{l}$.

The sequence parameters were adapted to the hardware solutions of the reference system. Correspondingly, a DF frequency of 25 kHz and a DF amplitude of 20 mT as well as an FF amplitude of 80 mT are assumed for all sequences. The common sequence time length T of 0.2 s and four densities S , ranging from 4 to 16, define the frequencies f_{FF} and f_{rot} summarised in Table 1. The choice of T leads to a memory requirement near the limit of our computer hardware. In order to simulate system matrices of trajectories where the FF frequency defines T , rotation frequencies above the reference system's upper limit of 5 Hz were allowed in the simulation.

For the two dimensional system matrix-based reconstruction, 10 iterations were performed with $\lambda = 10^{-4}$ and frequency selection by an SNR threshold of 2.

IV. Results

The results of the resolution study for the central and the outer right area are summarised in Figure 2. Results for the y -direction are not shown in favour of the x -direction since differences are negligible.

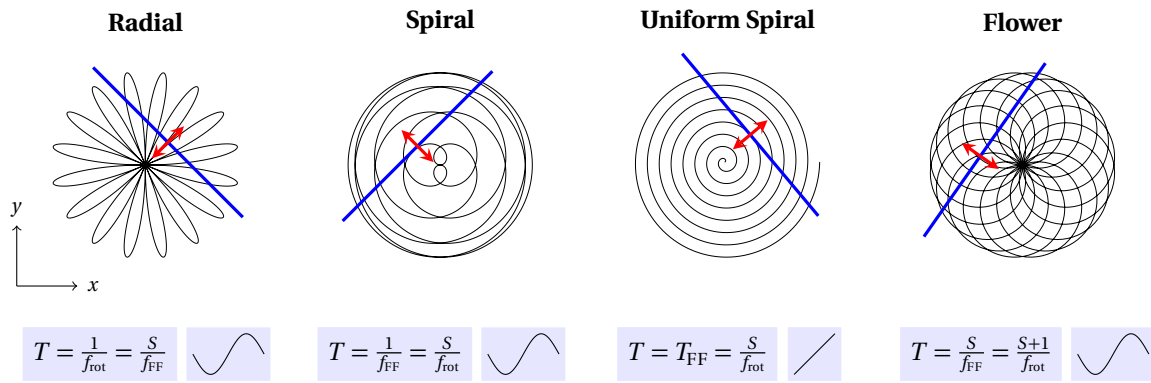


Figure 1: Trajectories traced by the FFL center with density $S = 8$. Each sequence is defined by a specific relation between the FF frequency f_{FF} ($T_{FF} = 1/f_{FF}$) and the rotation frequency of the FFL f_{rot} . These are related to the sequence time length T and the trajectory density S . Pictograms symbolise the FF current waveform being sinusoidal or ramp-shaped. The relative alignment of the FFL and the trajectory path is depicted by the solid blue line whereas the red arrow denotes the FFL movement due to the DF.

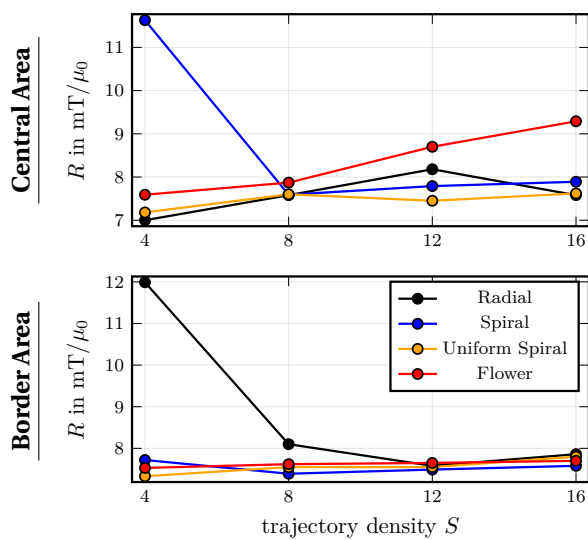


Figure 2: Spatial resolution R within a central area ($0 \text{ mT}/\mu_0$ offset) and a border area ($60 \text{ mT}/\mu_0$ offset).

The radial trajectory with density $S = 4$ yields the highest resolution in the center, whereas it shows the lowest resolution at the FOV edge. With increasing density, a homogeneous resolution of both areas is achieved. The spiral trajectory in turn shows for $S = 4$ the lowest resolution in the center region, while its resolution is comparatively high at the FOV border. An increase in trajectory density results in an increase of the uniformity of the spatial resolution. The uniform spiral trajectory provides a homogeneous resolution for all densities in both inspected areas. For low densities the flower trajectory shows a similar resolution behaviour, but an increase in density leads to a decrease in resolution at the center resulting in the comparatively lowest resolution for $S = 16$.

V. Discussion

The variation in resolution for all trajectories is attributed to a variable sampling density. An increasing trajectory density equals an increase in sampling density resulting in a mostly homogeneous resolution for $S = 16$. The low resolution of the center of the flower trajectory may be ascribed to an unfavourable choice of reconstruction parameters.

VI. Conclusion

With respect to the different trajectory densities, the uniform spiral trajectory is expected to provide the highest image quality, thus suitable for large FOV coverage. The radial trajectory showed the highest resolution of the center area, while the spiral trajectory yielded a high resolution of the border area making them suitable for sampling specific areas. An increase in trajectory density tended to improve the homogeneity of spatial resolution. Due to the integration of the framework algorithm [4], the developed simulation approach is already designed to calculate field sequenced signals based on real measurement data. Potentially, leveraging the framework from [4] the presented approach allows for more realistic FFL trajectory analysis in the future.

Acknowledgments

Research funding: The Fraunhofer IMTE is supported by the EU (EFRE) and the State Schleswig-Holstein, Germany (Project: IMTE – Grant: 124 20002/LPW-E1.1.1/1536).

References

- [1] M. Weber, J. Beuke, A. von Gladiss, K. Gräfe, P. Vogel, V. C. Behr, and T. M. Buzug. Novel field geometry using two halbach cylinders for ffl-mpi. *International Journal on Magnetic Particle Imaging*, 4(2):2019, 2018, doi:[10.18416/ijmpi.2018.1811004](https://doi.org/10.18416/ijmpi.2018.1811004).
- [2] C. B. Top, A. Güngör, S. Ilbey, and H. E. Güven. Trajectory analysis for field free line magnetic particle imaging. *Medical Physics*, 46(4):1592–1607, 2019, doi:[10.1002/mp.13411](https://doi.org/10.1002/mp.13411).
- [3] T. Knopp, S. Biederer, T. Sattel, J. Weizenecker, B. Gleich, J. Borgert, and T. Buzug. Trajectory analysis for magnetic particle imaging. *Physics in Medicine & Biology*, 54(2):385, 2008, doi:[10.1088/0031-9155/54/2/014](https://doi.org/10.1088/0031-9155/54/2/014).
- [4] F. Mohn, T. Knopp, M. Boberg, F. Thieben, P. Szwargulski, and M. Gräser. System matrix based reconstruction for pulsed sequences in magnetic particle imaging. *IEEE Transactions on Medical Imaging*, 2022, doi:[10.1109/TMI.2022.3149583](https://doi.org/10.1109/TMI.2022.3149583).
- [5] T. Knopp, P. Szwargulski, F. Griesse, M. Grosser, M. Boberg, and M. Möddel. Mpireco.jl: Julia package for image reconstruction in mpi. *International Journal on Magnetic Particle Imaging*, 5(1):9 pp, 2019, doi:[10.18416/ijmpi.2019.1907001](https://doi.org/10.18416/ijmpi.2019.1907001).
- [6] T. Knopp, S. Biederer, T. F. Sattel, M. Erbe, and T. M. Buzug. Prediction of the spatial resolution of magnetic particle imaging using the modulation transfer function of the imaging process. *IEEE transactions on medical imaging*, 30(6):1284–1292, 2011, doi:[10.1109/TMI.2011.2113188](https://doi.org/10.1109/TMI.2011.2113188).